Molecular Analyses of the Arabidopsis TUBBY-Like Protein Gene Family[1]

Chia-Ping Lai, Chang-Lung Lee, Po-Hsuan Chen, Shu-Hsing Wu, Chien-Chih Yang, and Jei-Fu Shaw*

Institute of Microbiology and Biochemistry, National Taiwan University, Taipei 106, Taiwan (C.-P.L., C.-C.Y.); Institute of Biochemistry, National Yang-Ming University, Shipai, Taipei 112, Taiwan (C.-L.L., J.-F.S.); and Institute of Botany, Academia Sinica, Nankang, Taipei 115, Taiwan (C.-P.L., P.-H.C., S.-H.W., J.-F.S.)

In mammals, TUBBY-like proteins play an important role in maintenance and function of neuronal cells during postdifferentiation and development. We have identified a TUBBY-like protein gene family with 11 members in Arabidopsis, named *AtTLP1-11*. Although seven of the *AtTLP* genes are located on chromosome I, no local tandem repeats or gene clusters are identified. Except for *AtTLP4*, reverse transcription-PCR analysis indicates that all these genes are expressed in various organs in 6-week-old Arabidopsis. *AtTLP1*, *2*, *3*, *6*, *7*, *9*, *10*, and *11* are expressed ubiquitously in all the organs tested, but the expression of *AtTLP5* and *8* shows dramatic organ specificity. These 11 family members share 30% to 80% amino acid similarities across their conserved C-terminal tubby domains. Unlike the highly diverse N-terminal region of animal TUBBY-like proteins, all AtTLP members except AtTLP8 contain a conserved F-box domain (51–57 residues). The interaction between AtTLP9 and ASK1 (Arabidopsis Skp1-like 1) is confirmed via yeast (*Saccharomyces cerevisiae*) two-hybrid assays. Abscisic acid (ABA)-insensitive phenotypes are observed for two independent *AtTLP9* mutant lines, whereas transgenic plants overexpressing *AtTLP9* are hypersensitive to ABA. These results suggest that *AtTLP9* may participate in the ABA signaling pathway.

The *TUBBY* gene was first identified from obese mice via positional cloning (Kleyn et al., 1996; Noben-Trauth et al., 1996). Mutation in the *tubby* gene causes maturity-onset obesity, insulin resistance, retinal degeneration, and neurosensory hearing loss (Coleman and Eicher, 1990; Heckenlively et al., 1995; Ohlemiller et al., 1995). In addition to TUBBY, four TUBBY related proteins, including TUBBY-like proteins (TULPs) 1 through 3 and TUBBY superfamily protein (TUSP), have since been identified in mammals (North et al., 1997; Nishina et al., 1998; Li et al., 2001). These proteins all feature an approximately 270-amino acid tubby domain at their C-terminal region, but their N-terminal sequences are more divergent both in length and in amino acid sequences. Mutations in this highly conserved C-terminal portion of mouse TUBBY and TULP1 lead to different deteriorated phenotypes (Kleyn et al., 1996; Noben-Trauth et al., 1996; North et al., 1997). Currently, members of this family have been identified in various multicellular organisms but not in single-celled organisms (North et al., 1997). The highly conserved tubby domain in different species suggests that these proteins must have fundamental biological functions in multicellular organisms.

Though target genes have not been identified, reports suggest that the TUBBY protein is a bipartite transcription regulator (Boggon et al., 1999). Santagata et al. (2001) showed that mouse TUBBY is transported from the plasma membrane to the nucleus after phospholipase C-β activation of a subclass of G proteins called $G\alpha_q$. Unlike the highly diverse N-terminal sequence of animal TULPs, a conserved F-box-containing domain is present in plant TUBBY-like protein (TLP) members (Gagne et al., 2002; Risseeuw et al., 2003). The F-box domain was first described as a sequence motif found in cyclin F that interacts with the protein S-phase kinase-associated protein 1 (SKP1) (Bai et al., 1996). Experimental data from work in yeast (*Saccharomyces cerevisiae*) indicate that SKP1 interacts with the CDC53 (Cullin) proteins and F-box proteins to form designated SKP1/Cullin/F-Box (SCF) complexes (E3 ubiquitin ligase complex; Krek, 1998; Patton et al., 1998).

F-box proteins can interact with SKP1-related proteins via an N-terminal F-box domain and with the substrates via a protein-protein interaction domain in C termini (Xiao and Jang, 2000). The review of the Arabidopsis F-box proteins suggests that most of the F-box domains are followed by specific amino acid sequences (such as the WD40 repeat, kelch repeats, and the Leu-rich repeat), which serve as protein-protein interacting domains for recruiting specific proteins and targeting them for ubiquitin mediated proteolysis (Patton et al., 1998; Xiao and Jang, 2000). Yeast F-box protein Grrlp of SCF^{Grrl} recruits phosphorylated Cln1 and Cln2 via Leu-rich repeats (Skowyra et al., 1999), and mammalian F-box protein β-TrCP of $SCF^{\beta\text{-TrCP}}$ recruits phosphorylated IkBd and β-catenin through WD40 repeats (Winston et al., 1999).

F-box proteins regulate diverse cellular processes, including cell cycle transition, transcriptional regu-

[1] This work was supported by a grant from the Genomic Program, Academia Sinica, Taipei, Taiwan.

* Corresponding author; e-mail boplshaw@gate.sinica.edu.tw; fax 886–2–27821605.

Article, publication date, and citation information can be found at www.plantphysiol.org/cgi/doi/10.1104/pp.103.037820.

lation, and signal transduction. Examples of F-box proteins regulating plant growth and development include TIR1 in auxin response (Rugger et al., 1998), UFO in floral organ identity determination (Samach et al., 1999), COI1 in jasmonic acid-regulated defense response (Xie et al., 1998), and ZTL and FKF1 in the control of the circadian clock (Somers et al., 2000; Nelson et al., 2000).

The existence of multiple TLPs implies their vital function in plants, though in-depth studies of plant TLPs have yet to be done. To reveal the potential functions of TLPs in plants, extensive bioinformatics and molecular characterization of TLPs in Arabidopsis were performed in this report. Using the yeast two-hybrid assays, we have confirmed that AtTLP9 is an F-box protein that can interact with ASK1 (Arabidopsis Skp1-like 1). At least one of the AtTLPs functions in the abscisic acid (ABA)-regulated pathway, based on the observation that transgenic plants with suppressed expression and overexpression of *AtTLP9* show aberrant sensitivity to ABA during seed germination and early seedling development.

RESULTS

Identification of the AtTLP Family

In the attempt to identify plant tubby domain-containing proteins, we used the tubby consensus sequence (Pfam PF01167) to search the Arabidopsis expressed sequence tag (EST) database and the completed Arabidopsis genome sequence. Our search revealed eleven TUBBY-like protein genes, termed *AtTLP1* to *AtTLP11*, in the Arabidopsis genome (Table I). For each of the 11 *AtTLP* genes, the corresponding bacterial artificial chromosome (BAC) locus (The Arabidopsis Information Resource), Tentative Consensus (TC) group, Arabidopsis Genome Initiative (AGI) gene code, cDNA GenBank accession number, and predicted protein length (no. of amino acid) are assembled in Table I.

Based on the sequence of predicted open reading frame and the corresponding EST in the database, gene-specific 5′ and 3′ primers were designed. When reverse transcription (RT)-PCR was performed with total RNA from 2-week-old Arabidopsis seedlings, 10 *AtTLP* cDNAs (*AtTLP1* to *3* and *AtTLP5* to *11*) were successfully amplified. Except for *AtTLP2* and *AtTLP11*, the amino acid sequences deduced from the *AtTLP1*, *AtTLP3*, *AtTLP5*, *AtTLP6*, *AtTLP7*, *AtTLP8*, *AtTLP9*, and *AtTLP10* cDNA sequences are identical to the predicted open reading frames in the database. Our *AtTLP2* cDNA sequence showed that intron 3 of *AtTLP2* was located between 708 and 781 bp, whereas the predicted splicing sites for this intron were 663 and 766 bp. Our *AtTLP11* cDNA sequence showed that intron 2 and intron 4 were located at 669 to 803 bp and 1,334 to 1,575 bp, respectively, whereas the computer predicted intron 2 was at 621 to 803 bp, and there is no predicted intron 4. cDNA sequences obtained from this study were submitted to GenBank (see Table I for accession nos.).

Sequence Analysis of the AtTLP Proteins

With the exception of AtTLP4 and 8, AtTLPs have a well-conserved tubby domain at their C termini. Unlike the highly diverse N-terminal sequence of animal TLUPs, a conserved F-box (51–57 residues)-containing domain (Pfam PF00646) is present in all AtTLP members except AtTLP8 (Fig. 1A). Among the AtTLP proteins, pairwise comparisons reveal that the tubby domains share 30% to 80% amino acid similarities (Fig. 1B). When analyzing the tubby domain in detail, we identified two PROSITE signature patterns as TUB1 (Prosite accession no. PS01200) and TUB2 motif (Prosite accession no. PS01201). The TUB1 and TUB2 motifs are located at the C terminus of AtTLPs and contain 14 and 16 amino acid residues, respectively. These two TUB motifs are highly conserved among the TLPs from various organisms. Though AtTLP4 and 8 do not have obvious signatures for

Table I. *Characteristics of AtTLP family members*

Gene Family Name	BAC Locus	TC Group	AGI Gene Code	cDNA GenBank Accession No.	Predicted Protein Length[a]
AtTLP1	F22K20.1	TC95487	At1g76900	AF487267	455
AtTLP2	T30D6.21	TC86308	At2g18280	AY045773	394
AtTLP3	F17A22.29	TC86633	At2g47900	AY045774	406
AtTLP4	F8K4.13	—	At1g61940	—	265
AtTLP5	T10P12.9	TC102456	At1g43640	AY046921	429
AtTLP6	F8G22.1	TC90700	At1g47270	AF487268	388
AtTLP7	F12M16.22	TC88599	At1g53320	AY092403	379
AtTLP8	T24D18.17	—	At1g16070	AF487269	397
AtTLP9	F24P17.15	TC102624	At3g06380	AF487270	380
AtTLP10	F4F7.13.	TC101291	At1g25280	AF487271	445
AtTLP11	T1A4.60	–	At5g18680	AY046922	380

[a]All the cDNAs of *AtTLP* genes, except *AtTLP4*, were cloned and sequenced to experimentally determine mRNA sequence; cDNAs were isolated and sequenced, and the encoded protein sequence was deduced from cDNA sequence.

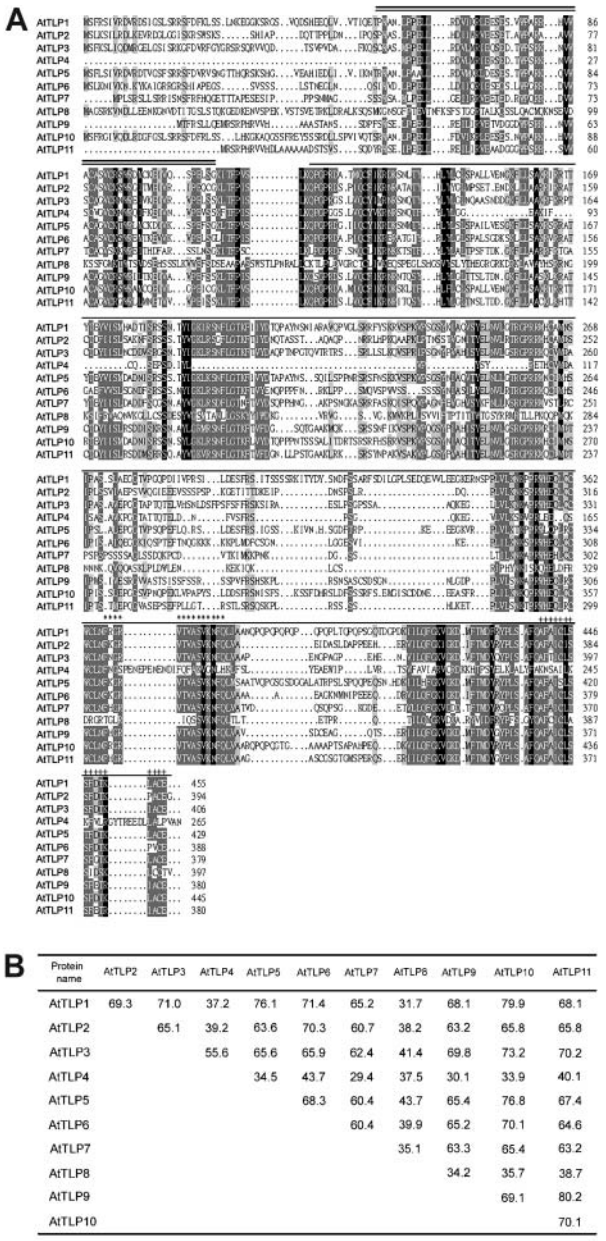

B

Protein name	AtTLP2	AtTLP3	AtTLP4	AtTLP5	AtTLP6	AtTLP7	AtTLP8	AtTLP9	AtTLP10	AtTLP11
AtTLP1	69.3	71.0	37.2	76.1	71.4	65.2	31.7	68.1	79.9	68.1
AtTLP2		65.1	39.2	63.6	70.3	60.7	38.2	63.2	65.8	65.8
AtTLP3			55.6	65.6	65.9	62.4	41.4	69.8	73.2	70.2
AtTLP4				34.5	43.7	29.4	37.5	30.1	33.9	40.1
AtTLP5					68.3	60.4	43.7	65.4	76.8	67.4
AtTLP6						60.4	39.9	65.2	70.1	64.6
AtTLP7							35.1	63.3	65.4	63.2
AtTLP8								34.2	35.7	38.7
AtTLP9									69.1	80.2
AtTLP10										70.1

Figure 1. Sequence comparisons of the deduced proteins from AtTLPs. A, Sequence alignment of AtTLPs. Identical and similar amino acid residues are shaded in black and gray, respectively. The locations of the F-box domain and tubby domain are indicated with double and single solid lines above the sequences, respectively. Asterisks and crosses shown above the sequences represent TUB1 and TUB2 motifs. Two PROSITE signature patterns are F-[KRHQ]-GR-V-[ST]-x-A-S-V-K-N-F-Q for TUB1 motif and A-F-[AG]-I-[GSAC]-[LIVM]-[ST]-S-F-x-[GST]-K-x-A-C-E for TUB2 motif. The amino acid sequences of AtTLP1-3 and AtTLP5-11 are deduced from the cDNAs reported here. The amino acid sequence of AtTLP4 is deduced from annotated At1g61940. The alignment is generated by the ClustalW program. The search for all known motifs in the deduced amino acid sequences was achieved by the MOTIF SCANNING (Pagni et al., 2001). B, Amino acid similarities among AtTLP C-terminal tubby domain.

TUB1 and TUB2 motifs, their C-terminal tubby domains are recognizable by MOTIF SCANNING (*N* score > 15; Pagni et al., 2001).

Location and Gene Structure Comparison of the *AtTLP* Gene Family

From the data in Figure 2A, the genes are obviously not evenly distributed in chromosomes I, II, III, or V. Seven genes (*AtTLP1*, *4*, *5*, *6*, *7*, *8*, and *10*) are located on chromosome I, whereas two genes (*AtTLP2* and *3*), one gene (*AtTLP9*), and one gene (*AtTLP11*) are located on chromosomes II, III, and V, respectively. Although

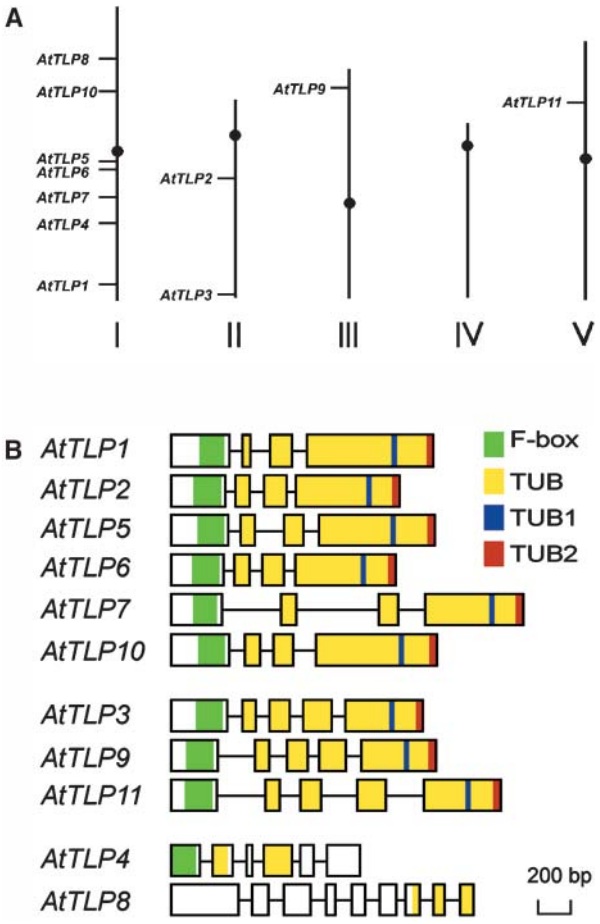

Figure 2. Location and gene structure comparison of the *AtTLP* gene family. A, Chromosomal locations of the *AtTLP* genes. The relative sizes of five Arabidopsis chromosomes are derived from the National Center for Biotechnology Information database. B, The intron-exon structure of the *AtTLP* gene family. Except for *AtTLP4,* the positions of the exons/introns of each individual *AtTLP* gene were confirmed by comparison of the cDNAs with their corresponding genomic DNA sequences. Exons and introns are represented by boxes and lines, respectively. The green and yellow shaded boxes indicate approximate positions encoding the F-box and tubby domain of the AtTLPs. Two PROSITE signature patterns (TUB1 and TUB2 motif) in tubby domain are shown in blue and red shaded boxes, respectively. The scale shown below is in base pairs.

most of the *AtTLP* genes are located on chromosome I, no local tandem repeats or gene clusters are identified.

By comparing the sequences of the RT-PCR products and the Arabidopsis genome, except for *AtTLP4*, the corrected exon-intron organization of the *AtTLP* genes is presented in Figure 2B. Gene structure indicates that the N-terminal leading sequences, the F-box, and the nine-residue spacer between the F-box and tubby domain are all located in exon 1, indicating that they might have arisen from the same ancestral gene. The C-terminal tubby domain sequences are distributed in exons interrupted by either two or three introns (Fig. 2B). On the basis of their exon and intron composition, the *AtTLP* genes can be classified into three groups. The genes of the first group (*AtTLP1*, *2*, *5*, *6*, *7*, and *10*) contain three introns. Members of the second group, *AtTLP3*, *9*, and *11*, contain an additional intron in the C-terminal region of the tubby domain. The third and most distinct group is composed of *AtTLP4* and *8*, containing five and eight introns, respectively.

Expression of *AtTLP* Genes

To understand how the expression of *AtTLP* gene family was regulated in different organs, total RNA from root, main and lateral stems, rosette leaves, flower clusters, and green siliques of soil-grown Arabidopsis were isolated for organ-specificity expression analyses of *AtTLP*s. Because the basal expression levels of *AtTLP*s were too low to be detected by RNA gel blotting with total RNA, we used coupled RT and PCR for the analysis. Results demonstrate that *AtTLP1*, *2*, *3*, *6*, *7*, *9*, *10*, and *11* are expressed in all the organs tested, with slight variations in mRNA accumulation (Fig. 3). By contrast, *AtTLP5* and *AtTLP8* primarily express in root, flower, and silique. The organ-specific expression of *AtTLP5* and *AtTLP8* may reflect their specific roles in particular organs.

Although the expression of *AtTLP1*, *2*, *3*, *6*, *7*, *9*, *10*, and *11* is omnipresent in tissues tested in this study, the possibility that these genes are expressed with cell-type specificity could not be excluded. It is also possible that differential expression of these *AtTLP* genes could only be observed when internal developmental programming was altered or specific environmental stimuli were applied to the plants. To test this hypothesis, we took advantage of the public Arabidopsis gene expression database at the Stanford Microarray Database, where hundreds of expression data sets based on cDNA microarray (http://genome-www5.stanford.edu/MicroArray/SMD/) are available. A search of the Arabidopsis EST database and the clone list used to generate Arabidopsis cDNA microarray revealed representative DNA elements corresponding to *AtTLP2*, *7*, *9*, and *10*. This allowed us to analyze the global gene expression pattern of these four genes by querying the microarray database. With the 2-fold expression difference cutoff, the expression profiles of these four genes are summarized in Table II. Results show factors like hormone fluctuation and environmental stimuli could modulate the expression of these four *AtTLP* genes.

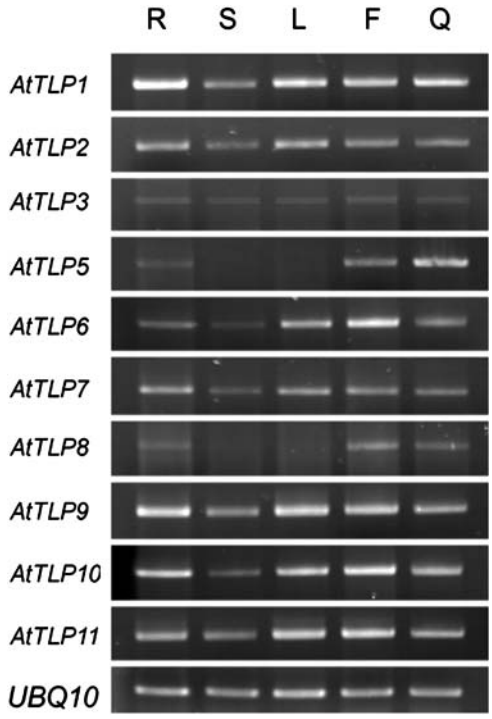

Figure 3. RT-PCR analyses of *AtTLP* gene expression patterns. Root (R), main and lateral stems (S), rosette leaves (L), flower clusters (F), and green siliques (Q) were harvested from 42-d-old plants grown in a growth chamber as described in "Materials and Methods." Expression of each *AtTLP* gene was analyzed by RT-PCR using specific primers as described in "Materials and Methods." The expression level of a *UBQ10* gene was used as an internal control.

The four *AtTLP* genes examined showed differential responses to treatments of various hormones. *AtTLP2* gene expression instantaneously increases more than 2-fold with cytokinin treatment but decreases to one-third when treated with indole-3-acetic acid. Cytokinin and auxin may play antagonistic roles in regulating *AtTLP2* gene expression. Another cytokinin-related experiment was aimed at identifying downstream genes of *KN1*. KN1-like protein is a homeobox transcription factor, the overexpression of which up-regulates cytokinin production and leads to delayed senescence (Vollbrecht et al., 1991). The expression of *AtTLP7* and *10* is up-regulated in *KN1* overexpression transgenic plant, while *AtTLP2* is down-regulated. The opposite response of *AtTLP7* from *AtTLP2* and *AtTLP9* to ABA treatment is also worth noticing. In *abscisic acid insensitive 1* mutant (Pei et al., 1997), the expression of *AtTLP2* and *AtTLP10* decreases 2- to 3-fold, but *AtTLP7* expression increases more than 2-fold. Interestingly, *AtTLP2* and *AtTLP7* respond oppositely to auxin treatment, *abscisic acid insensitive 1* mutant, and *KN1* overexpression transgenic plant. These two *AtTLP* genes may function antagonistically in regulating phytohormone signaling

Table II. *AtTLP gene expression analysis via searching microarray expression database*[a]

Experiment	Channel 1 Description	Channel 2 Description	Ch2/Ch1 Normalized (Mean)[b,c]			
			AtTLP2	*AtTLP7*	*AtTLP9*	*AtTLP10*
Hormone Effect						
Auxin response	msg[d] seedlings, untreated	msg seedlings; 10 μM indole-3-acetic acid for 30 min	0.32	2.21		
Auxin induction	Mock-treated Col-0 roots	Naphthylacetic acid-treated Col-0 roots		0.46		2.22
Cytokinin response	Control	15 min of cytokinin treatment	2.19			
Abscisic acid insensitive 1	Wild-type control	*Abscisic acid insensitive 1* mutant	0.49	2.6	0.35	
edr1 mutant	Wild-type leaves	*edr1* mutant leaves	2.33			
Downstream genes of *KN1*	Control	Overexpression of KN1-GR in Col-0 background	0.43	2.78		4.73
Stress						
Effects of elevated atmospheric CO_2	Col-0 leaves 360 ppm CO_2	Col-0 leaves 1,000 ppm CO_2	0.33			
Genes involved in chilling tolerance	Cold-treated Col-0 wild-type tissue	Cold-treated *cls8* mutant tissue	0.22		0.15	
Genes involved in potassium nutrition	[K+] = 120 μM	[K+] = 2 mM		0.34		0.2
Cadmium	Control	10 μM cadmium-treated plant			2.72	

[a]These data are obtained from http://genome-www5.stanford.edu. [b]All data are corresponding with fluorescence intensities greater than 500 in both channels and ch2:ch1 normalized ratio ≧2.0 or ≦0.5. [c]When searching dbEST with BLASTN, we find Arabidopsis EST corresponding to four of our *AtTLPs* represented on microarray data generated by AFGC. *AtTLP2* is corresponding to the EST clones 289B10T7 and 173K22T7. *AtTLP7*, *AtTLP9*, and *AtTLP10* are corresponding to the EST clones 173G1T7, 201E19T7, and F3E6T7, respectively. [d]It is the mutant of massugu gene, which has meanwhile been officially renamed to NPH4 (nonphototropic hypocotyl 4) gene.

pathways. The expression level of *AtTLP2* rises in the *edr1* (enhanced disease resistance 1) mutant leaves. *EDR1* gene encodes a putative MAP kinase similar to CTR1, a negative regulator of ethylene response in Arabidopsis (Frye et al., 2001). The *edr1* mutation of Arabidopsis also confers resistance to powdery mildew disease (Frye and Innes, 1998). The regulation of *AtTLP2* gene expression is possibly associated with salicylic acid-inducible and ethylene defense mechanism.

Environmental stresses also impose influences on the expression of *AtTLP* genes. For example, similar to the cold treatment on cls8 mutant, elevated concentration of CO_2 inhibits the expression of *AtTLP2*. K^+ deficiency augments the expression of *AtTLP7* and *AtTLP10* 3-fold and 5-fold, respectively. Heavy metal cadmium treatment also stimulates the expression of *AtTLP9* expression.

In conclusion, the expression data of these four *AtTLP* genes imply their potential involvement in phytohormone and environmental stress signaling. A comprehensive survey of *AtTLP* gene expression regulation upon hormone and stress treatment is expected to shed more light on this line of research but is beyond the scope of current studies.

AtTLP9 Can Interact with ASK1 Protein

Homology searches in the public databases reveal that TULPs are also present in multiple plant species (*Lemna paucicostata*, *Oryza sativa*, *Cicer arietinum*, *Zea mays*, and Arabidopsis). Unlike the highly diverse N-terminal sequence of animal TULPs, a conserved F-box-containing domain is present in plant TLP members. Sequence alignment of the F-box cores from AtTLP, TIR, UFO, COI1, and the human F-box protein Skp2 revealed conserved islands separated by regions

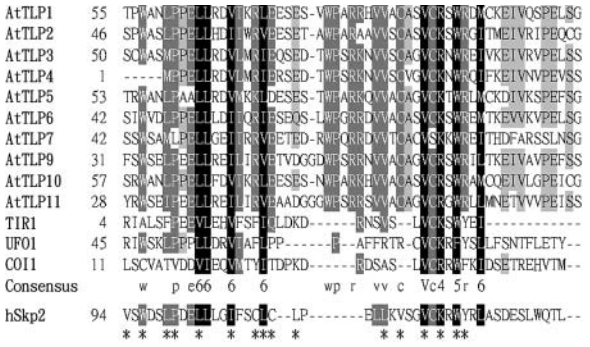

Figure 4. Sequence alignment of the core F-box sequences from AtTLPs, TIR1, UFO, COI1, and the human F-box protein Skp2 were aligned by ClustalW. The amino acid sequence of AtTLP4 is deduced from annotated At1g61940. Identical and similar amino acid residues are shaded with black and gray, respectively. Dots denote gaps. Amino acid substitution groups were numbered according to the Blosum 35 matrix: (1) ED; (2) NQ; (3) ST; (4) KR; (5) FYW; and (6) LIVM. Asterisks indicate the amino acids positions important for the Skp/F-box interactions between human Skp1 and Skp2 (Schulman et al., 2000; Zheng et al., 2002).

with weak homology (Fig. 4), but many of the conserved residues correspond with those known by x-ray crystallographic analysis to be important for Skp association (Schulman et al., 2000; Zheng et al., 2002). When members of AtTLP were aligned individually, the N-terminal F-box domain revealed highly conserved region (Fig. 1A). To test whether AtTLP could interact with the ASK1, one member of AtTLPs (AtTLP9) was chosen to test this hypothesis by yeast two-hybrid analysis. As shown in Figure 5, A and B, the acquiring of His biosynthesis and the presence of β-galactosidase activity suggested that AtTLP9 has physical interaction with ASK1.

Effect of ABA on the Seed Germination of *Attlp9* Mutants and Overexpression Lines

Based on the above observation that the expression of *AtTLP9* is altered in *abscisic acid insensitive 1* mutant and AtTLP9 could interact with ASK1, AtTLP9 was chosen in this study to investigate the putative in vivo functions of AtTLPs. Both loss-of-function and overexpression approaches were taken to address the biological role of AtTLP9. We obtained two AtTLP9 T-DNA insertion lines from the Arabidopsis Biological Resource Center (ABRC; SALK_016678 and 051138) and designated *attlp9-1* and *attlp9-2*, respectively. The insertion site of *attlp9-1* and *attlp9-2* were confirmed and are illustrated in Figure 6A. In brief, the mutant *attlp9-1* has a T-DNA insertion in the coding sequence at codon 705, whereas *attlp9-2* has an insertion in the 5′ distal region of this gene (Fig. 6A). The T-DNA insertion site of *attlp9-1* is identical to that originally described in SIGnAL; however, the T-DNA insertion site of *attlp9-2* is in the promoter region instead of exon 1 predicted in SIGnAL (the latter is supported by a potential full-length cDNA corresponding to At3g06380 generated in RIKEN; accession no. BT004092). Southern-blot analysis probed with *nptII* gene suggested one and three T-DNA insertion events in the T_4 *attlp9-1*and *attlp9-2* T-DNA insertion mutants, respectively (data not shown). Genotypes of *attlp9-1* and *attlp9-2* mutant lines were characterized both by their kanamycin resistance and genomic PCR with gene-specific primers and T-DNA left-border primer (Fig. 6, B and C). RT-PCR analyses of T_4 homozygous *attlp9-1* and *attlp9-2* plants showed that *attlp9-1* is a null allele, whereas *attlp9-2* is somewhat leaky (Fig. 6D).

We also generated transgenic plants with additional copy of *AtTLP9* cDNA driven by 35S promoter of cauliflower mosaic virus. From the transformation, we obtained 38 independent lines of transgenic plants (T_0 generation). Among them, we analyzed *AtTLP9* expression of seven independent homozygous lines from the T_3 sense transgenic plants in detail, as they contained a single copy of the transgene (data not shown). Two independent transgenic lines (S13-2 and S16-1), which showed dramatic increases in the endogenous level of *AtTLP9* transcript levels (Fig. 6E), were selected for more detailed analysis. As controls, a number of transgenic lines were generated by transforming with *Agrobacterium tumefaciens* with PBI121 vector alone.

The general development and growth phenotypes of the *attlp9-1* and *attlp9-2* knockout plants appear to be similar to those of the wild-type plants. However, when seeds were plated on nutrient agar media, the germination time of mutant *attlp9-1* and *attlp9-2* seeds was advanced several hours compared with that of the wild-type plants, whereas the selected sense line seeds germinated slightly later than vector control seeds (Fig. 7A). Seed germination is the outcome of

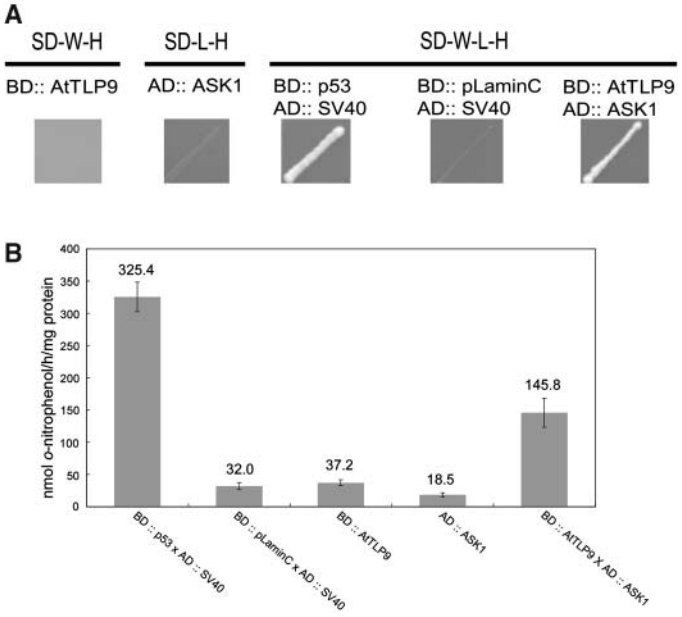

Figure 5. The interaction between AtTLP9 and ASK1 via yeast two-hybrid assays. p53-SV40 (SV40 T-antigen) and LaminC-SV40 represent known interacting and noninteracting protein partners, respectively. A, Interaction of AtTLP9 and ASK1 with yeast two-hybrid His auxotrophic growth. Yeast cells transformed with the plasmid pairs were cultured on synthetic dropout (SD) medium lacking selected amino acids. SD-W-H, SD media without Trp and His; SD-L-H, SD media without Leu and His; SD-W-L-H, SD media without Trp, Leu, and His. B, β-galactosidase activities of the interaction pairs. Values are the means ± SD of assays from least three independent transformants indicated. β-galactosidase activity is expressed in nmol *o*-nitrophenol h^{-1} mg^{-1} yeast protein.

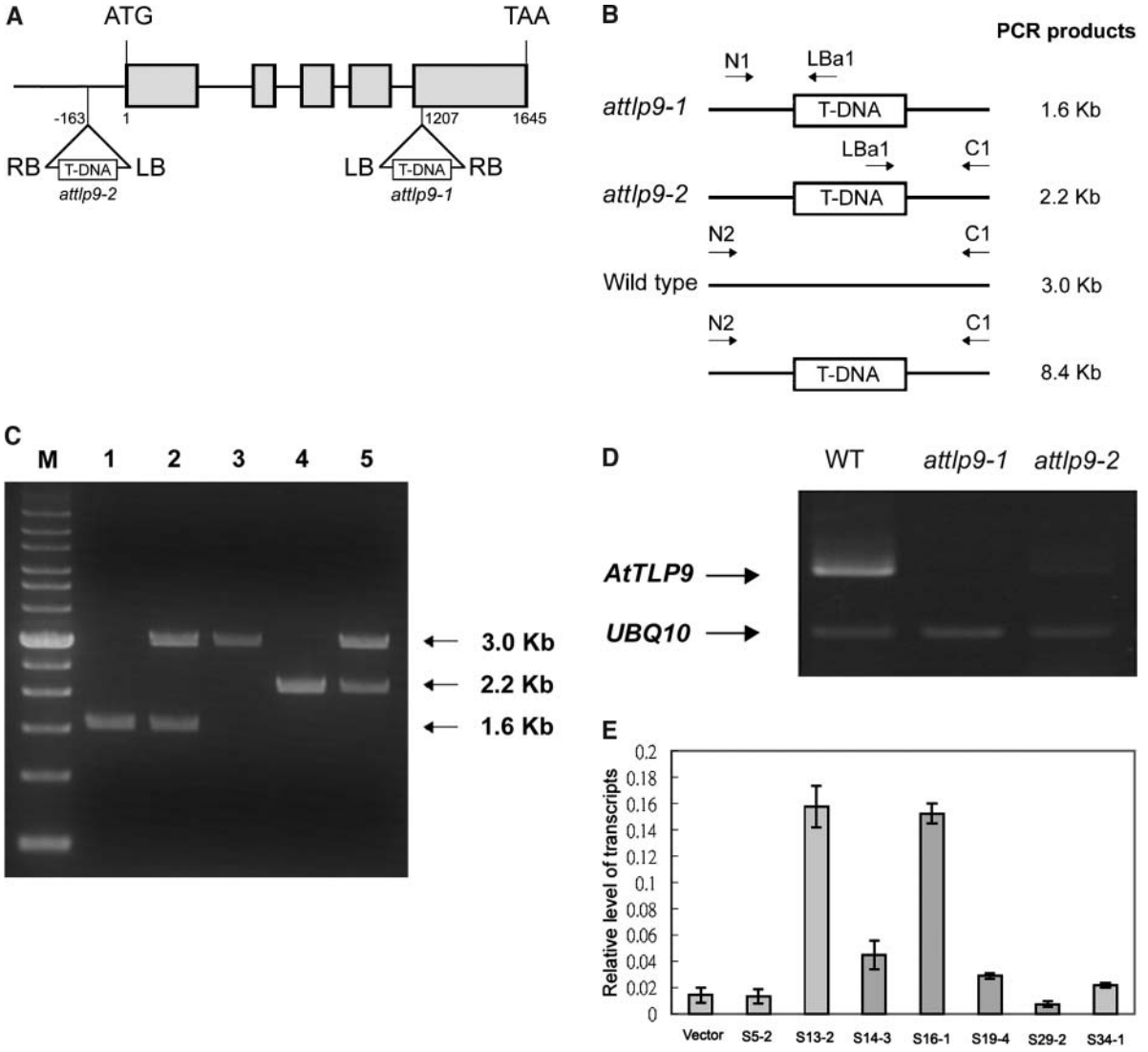

Figure 6. Molecular characterization of AtTLP9 T-DNA insertion lines. A, Schematic presentation of the structure of the *AtTLP9* genomic structure. Start ATG and termination codons are indicated. The five exons are represented by gray boxes. The T-DNA location for each of the two *attlp9* knockout lines, *attlp9-1* and *attlp9-2*, are indicated. B, Schematic diagrams of the *attlp9-1* and *attlp9-2* genotyping: N1, forward primer of *AtTULP9*; LBa1, left-border primer of T-DNA; and C1, reverse primer of *AtTLP9*. The N1 and LBa1 primers produced the 1.6-kb PCR fragment from the *attlp9-1* genomic DNA, and C1 and LBa1 primers produced the 2.2-kb PCR fragment from the *attlp9-2* T-DNA genomic DNA; N2 and C1 primers produced a 3.0-kb PCR product from the wild-type DNA, while no PCR band was obtained from the *attlp9-1* and *attlp9-2* genomic DNA because the expected fragment was too large to amplify. C, Genotype determination for *attlp9-1* and *attlp9-2*. Lane 1, homozygous *attlp9-1*; lane 2, heterozygous *attlp9-1*; lane 3, wild type; lane 4, homozygous *attlp9-2*; and lane 5, heterozygous *attlp9-2*. M, M_r marker. Size of major PCR products was indicated in kilobase pairs. D, Examination of *AtTLP9* transcript in *attlp9-1* and *attlp9-2* plants. RT-PCR was performed with total RNA extracted from 14-d-old seedlings of *attlp9-1*, *attlp9-2*, and the wild type (Col-0) as described in "Materials and Methods." UBQ10-specific primers were also included as an internal control. E, mRNA level for *AtTLP9* gene in 14-d-old seedlings of *AtTLP9* sense transgenic plants. Total RNA was extracted from 14-d-old seedlings of vector control and seven independent T_3 sense homozygous transgenic plants. Poly(A^+) mRNA was isolated, converted to cDNA, and subjected to real-time PCR analysis as described in "Materials and Methods." Transcript levels are given as relative values to *UBQ10* (the value of 1). Each data point represents the mean of triplicate experiments. The small bars represent SE. Vector represents transgenic plants carrying the empty vector.

an integration of many signals, coordinated by the interactions of stage-specific developmental regulators and the competing effects of hormonal signals (Finkelstein and Gibson, 2002). The most critical hormone promoting embryo maturation and preventing germination is ABA. To determine whether the transgenic plants display altered ABA responses, *AtTLP9* transgenic plants were germinated on media containing various concentrations of ABA. In the presence of 1 μM ABA, the germination of sense line

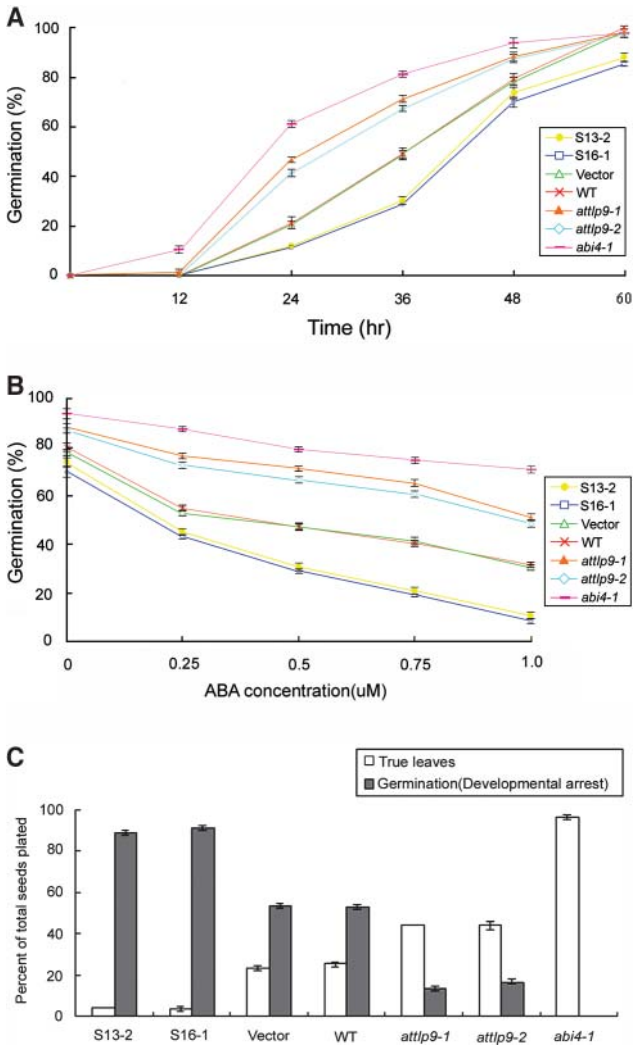

Figure 7. AtTLP9 can modulate plant's sensitivity to ABA during seed germination and early seedling development. WT, Columbia wild type; Vector, transgenic plants carrying the empty vector; *abi4-1*, ABA perception mutant. Plant material was prepared as described in "Materials and Methods." Each data point represents the mean of triplicate experiments ($n = 50$ each). The small bars represent SE. A, AtTLP9 can modulate the seed germination rate. Seeds of WT, *abi4-1*, *attlp9-1*, *attlp9-2*, and sense transgenic plants S13-2 and S16-1 were plated on ABA-free medium, and germination was scored at time points indicate. B, ABA dose response of seed germination. Seeds were plated on media containing various concentrations of ABA and grown for 2 d. Seedlings with fully emerged radicles were counted. C, Sensitivity of seedling development to ABA. Shown are the percentages of 10-d-old seedlings with developmental arrest and true leaves over total number of seeds planted on Murashige and Skoog media supplemented with 1 μM ABA and 1% Suc.

seeds was further delayed, and the germination rate was reduced to less than 10% (Fig. 7B). By contrast, the germination rate of *attlp9-1* and *attlp9-2* mutant seeds nearly reached 50%, and about 30% of wild-type seeds were able to germinate in the presence of 1 μM ABA. This suggests that the disruption of the *AtTLP9* gene affects the sensitivity of seeds to exogenous ABA. In addition to a reduced rate of seed germination, ABA also inhibited the growth and the greening process in cotyledons of the sense transgenic lines. In MS agar medium containing 1 μM ABA and 1% Suc, 90% of the 10-d-old seedlings showed developmental arrest, although the radicles of most sense lines seeds emerged (Fig. 7C). Under the same conditions, *attlp9-1* and *attlp9-2* plants continue to grow, and about 45% of the seedlings continue to develop true leaves, although at slower rates than *abi4-1* mutant does. These results indicate that the alteration of *AtTLP9* modulate plant's sensitivity to ABA during seed germination and early seedling development.

AtTLP9 Expression Is Transiently Up-Regulated during Imbibition of Seeds

Real-time PCR experiments were used to quantify AtTLP9 transcript levels at seed maturation, seed germination, and early development stage. During seed maturation and seed imbibition at 4°C for 72 h, *AtTLP9* transcripts remained at a relatively low level (Fig. 8). When the seeds were transferred to 22°C for further incubation, *AtTLP9* transcript levels rose in seeds after 8 h, reached the highest level at 16 h, and fell rapidly after 24 h, when the radicle emerged (Fig. 8). The *AtTLP9* transcripts were barely detectable afterward. We have shown that AtTLP9 is expressed early during germination and especially in the pre-emergent radicle.

DISCUSSION

In this study, we have defined and characterized a novel TUBBY-like protein gene family in Arabidopsis with a conserved tubby domain in their C-terminal region. Except for *AtTLP4*, the cDNAs of 10 *AtTLP*

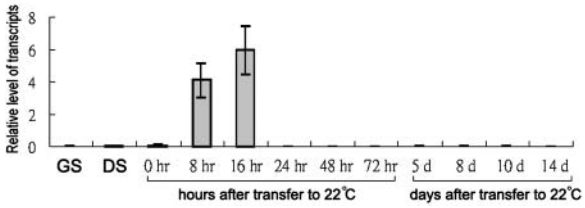

Figure 8. Real-time PCR analysis of AtTLP9 expression during seed maturation, germination, and early development. Wild-type (Col-0) seeds were kept in darkness at 4°C for 3 d, and then seeds for germination test were floated on liquid Murashige and Skoog medium and incubated at 22°C under a 16-h-light/8-h-dark photoperiod for 8, 16, 24, 48, and 72 h (0 indicates the time immediately following transfer), while seeds for early development test were plated on solid medium containing 0.7% phytoagar for 5, 8, 10, and 14 d. Poly(A^+) mRNA was isolated, converted to cDNA, and subjected to real-time PCR analysis as described in "Materials and Methods." Transcript levels are given as relative values to *UBQ10* (the value of 1). Each data point represents the mean of triplicate experiments. The small bars represent SE. GS, green siliques; DS, dry seeds.

genes are successfully obtained via RT-PCR. Our attempt to amplify the corresponding cDNA for *AtTLP4* via RT-PCR has been futile. The EST TC group for *AtTLP4* is also absent (Table I). It is possible that *AtTLP4* gene is not expressed or its transcript is too low to be detected with the experimental approaches undertaken to date. More work is needed to determine whether *AtTLP4* is indeed expressed or is a pseudogene.

An obvious feature of AtTLPs is the tubby domain. This highly conserved domain in different species suggests that these proteins must have fundamental biological functions in multicellular organisms. Three positively charged amino acid residues, R332, R363, and K330, are thought to be crucial for phosphatidylinositol 4,5-bisphosphate [PI (4,5) P_2] binding in the tubby domain of mouse TUBBY protein (Santagata et al., 2001). Except for AtTLP4 and 8, a sequence alignment of AtTLP tubby domain with mouse TUBBY protein reveals a putative PI (4,5) P_2 binding domain (data not shown). The presence of a conserved PI (4,5) P_2 binding domain in AtTLPs suggests that they may similarly bind to PI (4,5) P_2. Whether AtTLP can interact with PI (4,5) P_2, as has been observed in mammals, will be further investigated.

Experimental data show that TUBBY protein is a bipartite transcription regulator; the tubby domain of mouse TUBBY protein exhibits double-stranded DNA binding activity, and the N-terminal segment seems to modulate transcription (Boggon et al., 1999). In plants, the N-terminal region of TLPs is quite different from that in mammal TULPs. Unlike TUBBY and TULP1 in mouse, AtTLP9 fails to activate transcription from a GAL4 promoter when fused to the GAL4 DNA binding domain in a heterologous system (Fig. 5, A and B). However, further studies are needed to find out whether TLP plays a role as transcription factor in Arabidopsis.

Unlike the highly diverse N-terminal sequence of animal TULPs, all AtTLP members except AtTLP8 contain a conserved putative F-box domain (Fig. 4). Our data from yeast two-hybrid analysis showed that AtTLP9 can interact with ASK1 (Fig. 5, A and B). The F-box domain was first described as a sequence motif found in cyclin F that interacts with the protein SKP1 (Bai et al., 1996). Experimental data in yeast indicate that SKP1 interacts with the Cdc53 (Cullin) proteins and F-box proteins to form designated SCF complex (Krek, 1998; Patton et al., 1998). Analysis of the completed Arabidopsis genome sequence revealed 21 *Skp1*-like ASK genes that exhibit different expression patterns (Farrás et al., 2001; Zhao et al., 2003). Other studies demonstrated that ASK proteins exhibit differences in their association with both cullins and F-box proteins (Gagne et al., 2002; Risseeuw et al., 2003). ASK1, one of the 21 Skp proteins, is involved in both vegetative growth and reproductive development (Yang et al., 1999; Zhao et al., 1999, 2003). ASK1 was able to interact with one of several F-box proteins in yeast two-hybrid or in vitro-binding assays (del Pozo and Estelle , 1999; Dieterle et al., 2001; Gray et al., 2001; Woo et al., 2001; del Pozo et al., 2002; Gagne et al., 2002; Xu et al., 2002; Risseeuw et al., 2003). But the F-box domain alignment from the F-box proteins interacting with ASK1 showed poor conservation in an earlier (Risseeuw et al., 2003) and this study (Fig. 4). The best-studied role of F-box protein is a component of SCF complexes, which acts as a factor for substrate recognition (Pickart, 2001). In Arabidopsis, several SCF complexes have been characterized, such as SCF^{TIR1}, SCF^{COI1}, and SCF^{AtSKP2} (Gray et al., 1999; del Pozo et al., 2002; Xu et al., 2002). In *Caenorhabditis elegans* and yeast, it has been shown that SKP1 may form a complex lacking Cullin (Yamanaka et al., 2002; Stemmann et al., 2002). Whether AtTLP can form SCF complex will be further investigated by the coimmunoprecipitation experiment of AtTLP9 with CUL1 or RBX1.

To investigate the in vivo functions of AtTLPs, a representative member of the group II (AtTLP9) was selected for physiological study. Unlike *C. elegans*, *Drosophila melanogaster*, and mammals, plants appear to have relatively large numbers of TLPs (Nishina et al., 1998). According to the results in Table I, TLPs in Arabidopsis belong to a multigene family with 11 members. Functional redundancy within this family may mask the effects of an individual loss-of-function allele. To address this question, we also used gain-of-function approaches to generate overexpressed transgenic plants. Our analyses of these transgenic plants showed that *AtTLP9* overexpression and suppression affect sensitivity to ABA during seed germination and early seedling development. In Arabidopsis, ABA-insensitive mutations (e.g. *abi1*, *abi2*, *abi3*, *abi4*, and *abi5*) reduce seed dormancy and allow germination at ABA concentrations that are normally inhibitory to wild-type germination (Koornneef et al., 1984). Compared with *abi4-1*, our results indicate that the germination of *attulp9-1* knockout plants is weakly insensitive to ABA (Fig. 7, B and C). Seed germination can be divided into three phases, imbibition, increased metabolic activity, and initiation of growth, which loosely parallel the triphasic water uptake of dry mature seeds (Bewley, 1997). The transient expression of *AtTLP9* indicated that *AtTLP9* may function at stage II of seed germination as a checkpoint before radicle protrusion (Fig. 8). The exact mechanism of AtTLP9 function during seed germination will be further studied.

MATERIALS AND METHODS

Database Screening and Isolation AtTLP Genes cDNA Clones

Searching of the Arabidopsis database (The Institute of Genome Research) was performed with multiple BLAST algorithms to locate all the sequences sharing significant similarities with the tubby domain (Kleyn et al., 1996; Noben-Trauth et al., 1996; *P* value less than 0.0085). RT-PCR with gene-specific primers was performed to obtain cDNA clones for each *AtTLP* gene. To achieve this, total RNA from Arabidopsis tissues was isolated with Trizol

reagent (Invitrogen, Carlsbad, CA) according the manufacturer's suggestion. Poly(A^+) mRNA was isolated with oligo(dT)-coated magnetic beads and the PolyATract system (Promega, Madison, WI). First-strand cDNA was synthesized from 0.5 μg of poly(A^+) mRNA using SuperScript II RNase H RT (Invitrogen) according to the protocol of the supplier. For full-length cDNA amplification, the primer pairs used are as follows: AtTLP1-5′ (5′-ATGTCGTTCCGTAGCATAGTTCGT-3′), AtTLP1-3′ (5′-TTATTCGCAAGCAAGTTTTGTGTCG-3′), AtTLP2-5′ (5′-ATGTCTTTGAAAAGCATCCTTCGTGATC-3′), AtTLP2-3′ (5′-TTACCCTTCACATGCCGGTTTGGTGTCA-3′), AtTLP3-5′ (5′-ATGTCCTTCAAGAGTCTCATTCAG-3′), AtTLP3-3′ (5′-TCATTCACATGCTATCTTGGTGTC-3′), AtTLP5-5′ (5′-ATGTCGTTTCTGAGTATTGTTCG-3′), AtTLP5-3′ (5′-TTATTCACATGCCAATTTAGTAT-3′), AtTLP6-5′ (5′-ATGTCATTGAAGAACATAGTGAA-3′), AtTLP6-3′ (5′-TCATTCGCAGACTGGCTTCGTGT-3′), AtTLP7-5′ (5′-ATGCCTTTGTCACGGTCCCTC-3′), AtTLP7-3′ (5′-TCACTCGCAGGCAAGTTTAGTG-3′), AtTLP8-5′ (5′-ATGGCTGGTTCGAGAAAAGTGAA-3′), AtTLP8-3′ (5′-TCAAACAGTACAACAAAGCTTGG-3′), AtTLP9-5′ (5′-ATGACGTTCCGAAGTTTACTCCA-3′), AtTLP9-3′ (5′-TTATTCACAGGCAATTCTGGTTT-3′), AtTLP10-5′ (5′-ATGTCGTTTCGAGGCATTGTTCA-3′), AtTLP10-3′ (5′-CTATTCACAAGCAAGCTTGGTGT-3′), AtTLP11-5′ (5′-ATGTCGTTTCTGAGTATTGTTCG-3′), and AtTLP11-3′ (5′-TTATTCACATGCCAATTTAGTAT-3′).

Except for *AtTLP4* gene, gene-specific primer pairs were used for amplifying cDNA of each *AtTLP* gene from first-strand cDNA via PCR. PCR conditions were as follows: 3 min at 94°C followed by 25 cycles each of 1 min of denaturation at 94°C, 1 min of annealing at 55°C, and 1 min 30 s of extension at 72°C. The PCR products were purified with the QIAquick PCR purification kit (Qiagen, Valencia, CA) and subcloned into T-Easy vector (Promega). Each of these clones was sequence verified.

Bioinformatics

Chromosome localizations of the different *AtTLP* genes were analyzed by MapViewer (http://www.arabidopsis.org/servlets/mapper; Huala et al., 2001). The search for all known motifs in the deduced amino acid sequences was achieved by MOTIF SCANNING (Pagni et al., 2001). Multiple sequence alignment was performed with ClustalW (Thompson et al., 1994).

Expression Study

Spatial expression patterns of *AtTLP* genes were studied using a RT-PCR-based method. Total RNA was isolated from 42-d-old roots, main and lateral stems, rosette leaves, flower clusters, and green siliques. For each predicted gene or cDNA, a pair of gene-specific primers was chosen, and PCR amplifications were carried out using 15 ng of first-strand cDNA synthesized as described above. Primers of ubiquitin gene *UBQ10* (5′-ATTTCTCAAAATCTTAAAAACTT-3′ and 5′-TGATAGTTTTCC CAGTCAAC-3′) were used for an internal loading standard (Norris et al., 1993). Microarray database analysis was performed by searching the Arabidopsis Functional Genomics Consortium (AFGC) microarray expression database located at the Stanford Microarray Database (http://genome-www5.stanford.edu/MicroArray/SMD/; Wu et al., 2001).

Yeast Two-Hybrid Analysis

The yeast two-hybrid vectors pAD-*GAL4*-2.1 and pBD-*GAL4* Cam (Stratagene, La Jolla, CA), were used for C-terminal GAL4 AD and BD fusion constructions. A 1.1-kb *Sal*I-*Pst*I fragment containing the entire coding region of AtTLP9 was cloned into the *Sal*I-*Pst*I site of the pBD-*GAL4* Cam vector. A 480-bp *Eco*RI-*Pst*I fragment containing the entire coding region of ASK1 (At1g75950) was cloned into the *Eco*RI-*Pst*I site of the pAD-*GAL4*-2.1 vector. The yeast strain YRG-2 [MAT**a** *ura3-52 his3-200 ade2-101 lys2-801 trp1-901 leu2-3 112 gal4-542 gal80-538* LYS2::UAS_{GAL1}-$TATA_{GAL1}$-HIS3 URA3::$UAS_{GAL4\ 17mers(\times3)}$-$TATA_{CYC1}$-*lacZ*] was used in this study. The Y2H analysis was performed according to the manufacturer's recommendations (Stratagene).

Transgenic Lines

To identify *attlp9* T-DNA insertion mutant, we used AtTLP9 (At3g06380) to search the T-DNA Express database (http://signal.salk.edu/cgi-bin/tdnaexpress). Two putative *attlp9* T-DNA insertion mutants (ABRC seed stock SALK_016678 and 051138) were identified and designated *attlp9-1* and *attlp9-2*. T_3 seeds of *attlp9-1* and *attlp9-2* were obtained from the ABRC (Ohio State University, Columbus, OH). The position of the T-DNA within the *AtTLP9* was reconfirmed by sequencing the PCR-amplified fragment using pairs of primers corresponding to the T-DNA left borders and the *AtTLP9* gene-specific primer. The following primer pairs were used for *attlp9-1* and *attlp9-2* specific amplification: for *attlp9-1*, N1 (5′-ATGACGTTCCGAAGTTTACTC-3′) and LBa1 (5′-TGGTTCACGTAGTGGGCCATC-3′); for *attlp9-2*, C1 (5′-TTATTCACAGGCAATTCTGGT-3′) and LBa1 (5′-TGGTTCACGTAGTGGGCCATC-3′). The T-DNA of *attlp9-1* and *attlp9-2* carries a gene leading to resistance to kanamycin. Southern blot was probed with the *nptII* marker gene to determine the T-DNA insertion number in *attlp9-1* knockout mutant. Homozygous analyses of *attlp9-1* and *attlp9-2* plants were carried out by kanamycin selection and PCR method as described in Figure 5B. For the phenotype investigation, *attlp9-1* and *attlp9-2* T_4 homozygous lines were used for detailed analysis.

For the *35S::AtTLP9* sense construct, a gel-purified *Xba*I-*Sma*I fragment of AtTLP9 including the entire coding regions was inserted into an *Xba*I-*Sma*I site of the pBI121 Ti-vector (CLONTECH, Palo Alto, CA). The constructs were introduced into *Agrobacterium tumefaciens* strain LBA4404 by electroporation and transformed into wild-type plants by the floral dip method (Clough and Bent, 1998). For the phenotypic investigation, T_3 homozygous lines were used.

Plant Growth Conditions

The Arabidopsis ecotype Columbia-0 (Col-0) was used in this study. *abi4-1* was obtained from Dr. Wan-Hsing Cheng (Institute of Botany, Academia Sinica, Taipei, Taiwan). The phenotypes of *abi4-1* were confirmed as described (Söderman et al., 2000) prior to use. Seeds were surface sterilized with 70% ethanol for 30 s and then with 6% household bleach for 5 min before being washed five times with sterile water. For aseptic growth, they were then plated on solid medium containing Murashige and Skoog salts (Invitrogen), vitamins (Duchefa, Haarlem, The Netherlands), 0.7% phytoagar (Invitrogen), and 1% Suc and transferred to a tissue culture room. For soil growth, seedlings were transferred into individual pots 8 to 10 d after germination and maintained in the growth chamber. Plants were grown at 22°C under a 16-h-light/8-h-dark photoperiod aseptically or on soil.

To determine the sensitivity of germination to ABA, seeds collected at the same or similar times were used. After surface sterilization, sterile seeds were suspended in 0.15% agarose and kept in the dark at 4°C for 3 d to break residual dormancy. Then seeds were plated on agar plates in six replicates containing no ABA or 0.25, 0.5, 0.75, or 1.0 μM ABA in 12-cm plastic petri dishes. Each agar plate was divided into seven halves, and 50 seeds of wild-type and AtTLP9 transgenic seeds were plated on each part. A seed was regarded as germinated when the radicle protruded through the seed coat.

Real-Time PCR

The relative expression of *AtTLP9* was measured using real-time PCR on the ABI PRISM 7700 sequence detection system (Applied Biosystems, Scoresby, Victoria, Australia). *UBQ10* was used as the endogenous control (Norris et al., 1993).

Primers were designed using Primer Express 1.0 software (Applied Biosystems, Foster City, CA). The primers used were: AtTLP9 forward primer, 5′-TAGGCCACACCGTGTAGTTCA-3′; AtTLP9 reverse primer, 5′-CGTCAACAGTCTCAACCCTAATCA-3′; UBQ10 forward primer, 5′-AGAAGTTCAATGTTTCGTTTCATGTAA-3′; and UBQ10 reverse primer, 5′-GAACGGAAACATAGTAGAACACTTATTCA-3′.

The real-time PCR was performed in 50 μL of reaction mixture containing 500 ng first-strand cDNA, 2.5 μM each primer, and 1× SYBR Green PCR Master Mix (Applied Biosystems). PCR cycling was 50°C for 2 min, 95°C for 10 min, followed by 40 cycles of 15 s at 95°C and 1 min at 60°C. The *UBQ10* mRNA quantity was set at 1, and *AtTLP9* expression was determined relative to control samples. Threshold cycles were determined using Sequence Detection System version 1.7a software (Applied Biosystems) for all results.

Sequence data from this article have been deposited with the EMBL/GenBank data libraries under accession numbers AF487267, AY045773, AY045774, AY046921, AF487268, AY092403, AF487269, AF487270, AF487271, and AY046922.

ACKNOWLEDGMENTS

We thank Miss May-Chih Fen, Institute of Botany, Academia Sinica, for DNA sequencing. We also thank Professor Anthony Huang of University of California, Riverside; Professor Tuan-hua David Ho of Academia Sinica; and Professor Teh-hui Kao of Penn State University for their critical reading of this manuscript. We thank the Salk Institute Genomic Analysis Laboratory for providing the sequence-indexed Arabidopsis T-DNA insertion mutants and ABRC for providing seeds of *attlp9-1* and *attlp9-2*.

Received December 18, 2003; returned for revision January 29, 2004; accepted January 29, 2004.

LITERATURE CITED

Bai C, Sen P, Hofmann K, Ma L, Goebl M, Harper JW, Elledge SJ (1996) SKP1 connects cell cycle regulators to the ubiquitin proteolysis machinery through a novel motif, the F-box. Cell **86:** 263–274

Bewley JD (1997) Seed germination and dormancy. Plant Cell **9:** 1055–1066

Boggon TJ, Shan WS, Santagata S, Myers SC, Shapiro SL (1999) Implication of tubby proteins as transcription factors by structure-based functional analysis. Science **286:** 2119–2125

Clough SJ, Bent AF (1998) Floral dip: a simplified method for Agrobacterium-mediated transformation of Arabidopsis thaliana. Plant J **16:** 735–743

Coleman DL, Eicher EM (1990) Fat (fat) and tubby (tub): two autosomal recessive mutations causing obesity syndromes in the mouse. J Hered **81:** 424–427

del Pozo JC, Boniotti MB, Gutierrez C (2002) Arabidopsis E2Fc functions in cell division and is degraded by the ubiquitin-SCF(AtSKP2) pathway in response to light. Plant Cell **14:** 3057–3071

del Pozo JC, Estelle M (1999) The Arabidopsis cullin AtCUL1 is modified by the ubiquitin-related protein RUB1. Proc Natl Acad Sci USA **96:** 15342–15347

Dieterle M, Zhou YC, Schafer E, Funk M, Kretsch T (2001) EID1, an F-box protein involved in phytochrome A-specific light signaling. Genes Dev **15:** 939–944

Farrás R, Ferrando A, Jasik J, Kleinow T, Okresz L, Tiburcio A, Salchert K, del Pozo C, Schell J, Koncz C (2001) SKP1-SnRK protein kinase interactions mediate proteasomal binding of a plant SCF ubiquitin ligase. EMBO J **20:** 2742–2756

Finkelstein RR, Gibson SI (2002) ABA and sugar interactions regulating development: cross-talk or voices in a crowd? Curr Opin Plant Biol **5:** 26–32

Frye CA, Innes RW (1998) An Arabidopsis mutant with enhanced resistance to powdery mildew. Plant Cell **10:** 947–956

Frye CA, Tang D, Innes RW (2001) Negative regulation of defense responses in plants by a conserved MAPKK kinase. Proc Natl Acad Sci USA **98:** 373–378

Gagne JM, Downes BP, Shiu SH, Durski AM, Vierstra RD (2002) The F-box subunit of the SCF E3 complex is encoded by a diverse superfamily of genes in Arabidopsis. Proc Natl Acad Sci USA **99:** 11519–11524

Gray WM, del Pozo JC, Walker L, Hobbie L, Risseeuw E, Banks T, Crosby WL, Yang M, Ma H, Estelle M (1999) Identification of an SCF ubiquitin ligase complex required for auxin response in *Arabidopsis thaliana*. Genes Dev **13:** 1678–1691

Gray WM, Kepinski S, Rouse D, Leyser O, Estelle M (2001) Auxin regulates SCF^{TIR1}-dependent degradation of AUX/IAA proteins. Nature **414:** 271–276

Heckenlively JR, Chang B, Erway LC, Peng C, Hawes NL, Hageman GS, Roderick TH (1995) Mouse model for usher syndrome: linkage mapping suggests homology to usher type I reported at human chromosome 11p15. Proc Natl Acad Sci USA **92:** 11100–11104

Huala E, Dickerman AW, Garcia-Hernandez M, Weems D, Reiser L, LaFond F, Hanley D, Kiphart D, Zhuang M, Huang W, et al (2001) The Arabidopsis Information Resource (TAIR): a comprehensive database and web-based information retrieval, analysis, and visualization system for a model plant. Nucleic Acids Res **29:** 102–105

Kleyn PW, Fan W, Kovats SG, Lee JJ, Pulido JC, Wu Y, Berkemeier LR, Misumi DJ, Holmgren L, Charlat O, et al (1996) Identification and characterization of the mouse obesity gene tubby: a member of a novel gene family. Cell **85:** 281–290

Koornneef M, Reuling G, Karssen CM (1984) The isolation and characterization of abscisic acid-insensitive mutants of *Arabidopsis thaliana*. Physiol Plant **61:** 377–383

Krek W (1998) Proteolysis and the G1-S transition: the SCF connection. Curr Opin Genet Dev **8:** 36–42

Li QZ, Wang CY, Shi JD, Ruan QG, Eckenrode S, Davoodi-Semiromi A, Kukar T, Gu Y, Lian W, Wu D, et al (2001) Molecular cloning and characterization of the mouse and human TUSP gene, a novel member of the tubby superfamily. Gene **273:** 275–284

Nelson DC, Lasswell J, Rogg LE, Cohen MA, Bartel B (2000) FKF1, a clock-controlled gene that regulates the transition to flowering in Arabidopsis. Cell **101:** 331–340

Nishina PM, North MA, Ikeda A, Yan Y, Naggert JK (1998) Molecular characterization of a novel tubby gene family member, TULP3, in mouse and humans. Genomics **54:** 215–220

Noben-Trauth K, Naggert JK, North MA, Nishina PM (1996) A candidate gene for the mouse mutation tubby. Nature **380:** 534–538

North MA, Naggert JK, Yan Y, Noben-Trauth K, Nishina PM (1997) Molecular characterization of TUB, TULP1, and TULP2, members of the novel tubby gene family and their possible relation to ocular diseases. Proc Natl Acad Sci USA **94:** 3128–3133

Norris SR, Meyer SE, Callis J (1993) The intron of polyubiquitin genes is conserved in location and is a quantitative determinant of chimeric gene expression. Plant Mol Biol **21:** 895–906

Ohlemiller KK, Hughes RM, Mosinger-Ogilvie J, Speck JD, Grosof DH, Silverman MS (1995) Cochlear and retinal degeneration in the tubby mouse. Neuroreport **6:** 845–849

Pagni M, Iseli C, Junier T, Falquet L, Jongeneel V, Bucher P (2001) TrEST, trGEN and Hits: access to databases of predicted protein sequences. Nucleic Acids Res **29:** 148–151

Patton EE, Willems AR, Tyers M (1998) Combinatorial control in ubiquitin-dependent proteolysis: Don't Skp the F-box hypothesis. Trends Genet **14:** 236–243

Pei ZM, Kuchitsu K, Ward JM, Schwarz M, Schroeder JI (1997) Differential abscisic acid regulation of guard cell slow anion channels in Arabidopsis wild-type and *abi1* and *abi2* mutants. Plant Cell **9:** 409–423

Pickart CM (2001) Mechanisms underlying ubiquitination. Annu Rev Biochem **70:** 503–533

Risseeuw EP, Daskalchuk TE, Banks TW, Liu E, Cotelesage J, Hellmann H, Estelle M, Somers DE, Crosby WL (2003) Protein interaction analysis of SCF ubiquitin E3 ligase subunits from Arabidopsis. Plant J **34:** 753–767

Rugger M, Dewey E, Gray WM, Hobbie L, Turner J, Estelle M (1998) The TIR1 protein of Arabidopsis functions in auxin response and is related to human SKP2 and yeast grr1p. Genes Dev **12:** 198–207

Samach A, Llenz JE, Kohalmi SE, Risseeuw E, Haughn GW, Grosby WL (1999) The UNUSUAL FLORAL ORGANS gene of Arabidopsis thaliana is an F-box protein required for normal patterning and growth in the floral meristem. Plant J **20:** 433–445

Santagata S, Boggon TJ, Baird CL, Gomez JA, Zhao J, Shan WS, Myszka DG, Shapiro SL (2001) G-protein signaling through tubby proteins. Science **292:** 2041–2050

Schulman BA, Carrano AC, Jeffrey PD, Bowen Z, Kinnucan ER, Finnin MS, Elledge SJ, Harper JW, Pagano M, Pavletich NP (2000) Insights into SCF ubiquitin ligases from the structure of the Skp1-Skp2 complex. Nature **408:** 381–386

Skowyra D, Koepp DM, Kamura T, Conrad MN, Conaway RC, Conaway JW, Elledge SJ, Harper JW (1999) Reconstitution of G1 cyclin ubiquitination with complexes containing SCFGrr1 and Rbx1. Science **284:** 662–665

Söderman EM, Brocard IM, Lynch TJ, Finkelstein RR (2000) Regulation and function of the Arabidopsis *ABA-insensitive4* gene in seed and abscisic acid response signaling networks. Plant Physiol **124:** 1752–1765

Somers DE, Schultz TF, Milnamow M, Kay SA (2000) *ZEITLUPE* encodes a novel clock-associated PAS protein from Arabidopsis. Cell **101:** 319–329

Stemmann O, Neidig A, Kocher T, Wilm M, Lechner J (2002) Hsp90 enables Ctf13p/Skp1p to nucleate the budding yeast kinetochore. Proc Natl Acad Sci USA **99:** 8585–8590

Thompson JD, Higgins DG, Gibson TJ (1994) CLUSTALW: improving the sensitivity of progressive weighting, position-specific gap penalties and weight matrix choice. Nucleic Acids Res **22:** 4673–4680

Vollbrecht E, Veit B, Sinha N, Hake S (1991) The developmental gene Knotted-1 is a member of a maize homeobox gene family. Nature **350:** 241–243

Winston JT, Strack P, Beer-Romero P, Chu CY, Elledge SJ, Harper JW (1999) The SCFbeta-TRCP-ubiquitin ligase complex associates specifically with phosphorylated destruction motifs in IkappaBalpha and beta-catenin and stimulates IkappaBalpha ubiquitination in vitro. Genes Dev **13:** 270–283

Woo HR, Chung KM, Park JH, Oh SA, Ahn T, Hong SH, Jang SK, Nam HG (2001) ORE9, an F-box protein that regulates leaf senescence in Arabidopsis. Plant Cell **13:** 1779–1790

Wu SH, Ramonell K, Gollub J, Somerville SC (2001) Plant gene expression profiling with DNA microarrays. Plant Physiol Biochem **39:** 917–926

Xiao W, Jang J (2000) F-box proteins in Arabidopsis. Trends Plant Sci **5:** 454–457

Xie DX, Feys BF, James S, Nieto-Rostro M, Turner JG (1998) COI1: an Arabidopsis gene required for jasmonate-regulated defense and fertility. Science **280:** 1091–1094

Xu L, Liu F, Lechner E, Genschik P, Crosby WL, Ma H, Peng W, Huang D, Xie D (2002) The SCF^{COI1} ubiquitin-ligase complexes are required for jasmonate response in Arabidopsis. Plant Cell **14:** 1919–1935

Yamanaka A, Yada M, Imaki H, Koga M, Ohshima Y, Nakayama KI (2002) Multiple Skp1-related proteins in *Caenorhabditis elegans*: diverse patterns of interaction with Cullins and F-Box proteins. Curr Biol **12:** 267–275

Yang M, Hu Y, Lodhi M, McCombie WR, Ma H (1999) The *Arabidopsis SKP1-LIKE1* gene is essential for male meiosis and may control homologue separation. Proc Natl Acad Sci USA **96:** 11416–11421

Zhao D, Ni W, Feng B, Han T, Petrasek MG, Ma H (2003) Members of the *Arabidopsis-SKP1-like* gene family exhibit a variety of expression patterns and may play diverse roles in Arabidopsis. Plant Physiol **133:** 203–217

Zhao D, Yang M, Solava J, Ma H (1999) The *ASK1* gene regulates development and interacts with the *UFO* gene to control floral organ identity in *Arabidopsis*. Dev Genet **25:** 209–223

Zheng N, Schulman BA, Song L, Miller JJ, Jeffrey PD, Wang P, Chu C, Koepp DM, Elledge SJ, Pagano M, et al (2002) Structure of the Cul1-Rbx1-Skp1-F box Skp2 SCF ubiquitin ligase complex. Nature **416:** 703–709